Biomaterials Science

ROYAL SOCIETY OF CHEMISTRY

PAPER

View Article Online
View Journal | View Issue

Cite this: *Biomater. Sci.*, 2023, **11**, 2405

A natural polyphenol-functionalized chitosan/gelatin sponge for accelerating hemostasis and infected wound healing†

Yujie Sun,‡[a] Tengfei Miao,‡[b,c] Yu Wang,‡[b,c] Xiaochen Wang,[d] Jie Lin,[b,c] Nana Zhao,[b,c] Yang Hu*[b,c] and Fu-Jian Xu*[b,c]

Natural polymers have been particularly appealing for constructing hemostatic materials/devices, but it is still desirable to develop new natural polymer-based biomaterials with balanced hemostatic and wound-healing performance. In this work, a natural polyphenol-functionalized chitosan/gelatin sponge (PCGS) was prepared by the lyophilization of a chitosan/gelatin mixture solution (under a self-foaming condition to prepare the CGS) and subsequent chemical cross-linking with procyanidin (PC). Compared with the original CGS, PCGS exhibited an enhanced liquid-absorption ability, reduced surface charges, and similar/low hemolysis rate. Benefiting from such a liquid-absorption ability (~4000% for whole blood and normal saline) and moderate surface charges, PCGS exhibited high *in vitro* hemostatic property and promising hemostatic performance in an *in vivo* femoral-artery-injury model. In addition, PCGS possessed higher antioxidant property and slightly decreased antibacterial ability than CGS, owing to the incorporation of PC. The feasibility of PCGS for treating infected wounds was further confirmed in an *in vivo* infected-tooth-extraction model, as the typical complication of intractable tooth-extraction bleeding. The present work demonstrated a facile approach for developing multifunctional hemostatic materials through the flexible management of natural polymers and polyphenols.

Received 14th December 2022,
Accepted 2nd February 2023

DOI: 10.1039/d2bm02049a

rsc.li/biomaterials-science

1. Introduction

Hemostasis is a major point of emergency treatment for severe trauma caused by traffic accidents, natural disasters, and complicated operations.[1–3] Hemostatic materials have been explored as a key assistant to surgical techniques for uncontrolled/intractable bleeding. Owing to their excellent biocompatibility, low immunogenicity, and varied bioactivity,[4,5] natural polymers (*i.e.*, starch, cellulose, gelatin, and chitosan) have been particularly appealing for constructing hemostatic materials in both research work and clinical trials. However, the clinically used hemostatic devices, including the cellulose-based Surgicel hemostat and starch-based Arista hemostatic powder,[1] have been reported with high biosafety but are associated with single, unsatisfactory hemostatic performance. There have been other natural polymer-based materials developed as possible substitutes of these hemostatic devices.[6–10] Among them, sponges have been a common type used in hemostatic materials/devices[11–14] and are designed to absorb blood from wounds, concentrate blood components, and accelerate the clotting process. Most conventional hemostatic sponges either only achieve a limited liquid-adsorption property (low adsorption ratio or slow speed, difficult to effect quick hemostasis) or rely on an elaborate chemical synthesis (far from large-scale production clinical use). Therefore, it is still desirable to develop a facile approach for natural polymer-based hemostatic sponges with high hemostatic performance.

Tooth-extraction bleeding (TEB) is a recognized, frequently encountered complication in dental practice.[15] After tooth exaction, soft tissue tearing, granulation tissue remnant, vascular rupture, and alveolar process fracture can induce TEB.[16] A reasonable selection and local application of hemostatic materials/devices are the main strategy to prevent/treat TEB and decrease the pain of the patients.[17] Notably, the oral cavity is an open bacterial environment and tooth extraction is an invasive surgical operation, which can easily lead to oral

[a]*Department of Dental Implant Center, Beijing Stomatological Hospital, School of Stomatology, Capital Medical University, Beijing 100050, China*
[b]*Key Lab of Biomedical Materials of Natural Macromolecules (Beijing University of Chemical Technology, Ministry of Education), Beijing Laboratory of Biomedical Materials, Beijing University of Chemical Technology, Beijing, 100029, China. E-mail: xufj@mail.buct.edu.cn, huyang@mail.buct.edu.cn*
[c]*College of Materials Science and Engineering, Beijing University of Chemical Technology, Beijing 100029, PR China*
[d]*Shandong Center for Food and Drug Evaluation & Inspection, Jinan 250014, China*
†Electronic supplementary information (ESI) available. See DOI: https://doi.org/10.1039/d2bm02049a
‡These authors contributed equally.

wound infection/infectious inflammation after tooth extraction. Therefore, excessive (too rapid) hemostasis by hemostats without anti-infection function can weaken the antibacterial/anti-inflammatory property of the body's socket blood (containing plenty of immune cells and anti-inflammatory factors), interrupt the normal healing after tooth extraction, and even generate a chronic wound called "dry socket".[18,19] To address TEB and other intractable bleedings that are associated with the complicated healing process, it is highly desirable to develop multifunctional hemostatic materials with balanced hemostatic and antibacterial/anti-inflammatory properties.

In this work, chitosan/gelation composite sponges (CGSs) were first prepared by the lyophilization of mixed chitosan and gelatin solutions in different ratios (Fig. 1). A facile 'green' self-foaming condition was realized by the vigorous stirring of high-viscosity solutions in the presence of amphiphilic gelatin (without extra foaming agent), in order to endow the CGS with a highly porous morphology. Procyanidin (PC), a naturally occurring polyphenol with high antioxidant and antibacterial properties,[20,21] was adopted for the cross-linking of the CGSs *via* an efficient Schiff base reaction to prepare PC-functionalized CGS (PCGS). The incorporation of PC in the PCGS was proposed to not only reinforce their porous morphology for a higher liquid-adsorption property, but also endow antioxidant property for better wound healing. The optimal PCGS was screened from sponges with different chitosan/gelatin/PC components through their performance in various *in vitro* hemostatic, antioxidant, and antibacterial assays. The feasibility of PCGS for treating severe or intractable bleeding was investigated in detail, including in an *in vivo* femoral-artery-injury

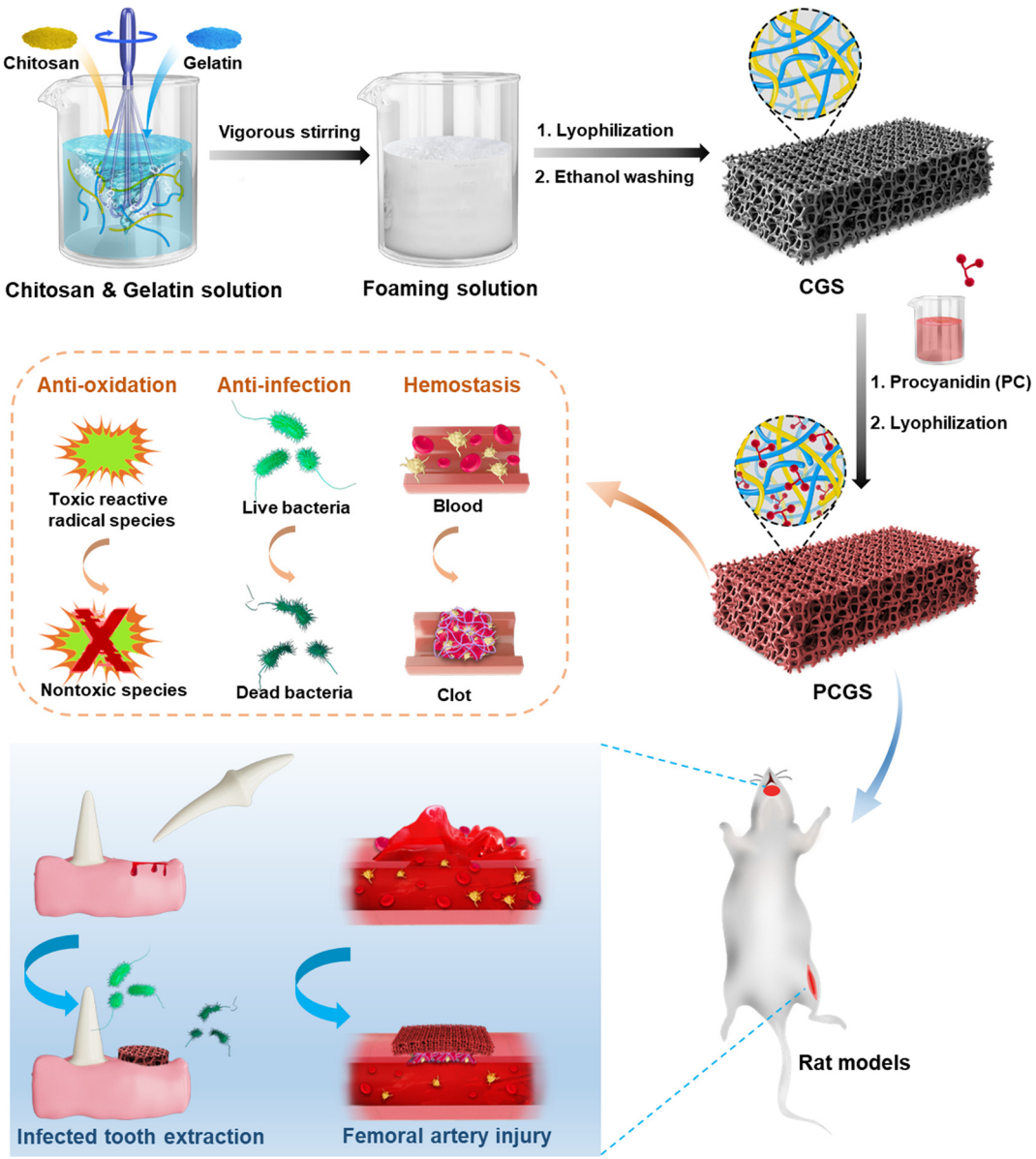

Fig. 1 Schematic illustration of the preparation of PCGS for hemostatic and infected wound therapy.

model (for accelerating hemostasis in hemorrhage control) and *in vivo* infected-tooth-extraction model (for accelerating infected oral wound healing as the typical complication of intractable TEB).

2. Experimental section

2.1. Materials

Chitosan (degree of deacetylation of 95%, extracted from shrimp and crab shell) was purchased from Qingdao Huizhi Biotechnology Co., Ltd (China). Procyanidin (PC, 99%, extracted from grape seed) was obtained from Xi'an Wanfang Biotechnology Co., Ltd (China). Gelatin [gel strength of 160–190 Bloom g (determined by 6.67%/10 °C), extracted from porcine skin] was obtained from Rousselot (Wenzhou) Gelatin Co., Ltd (China). Tris(hydroxymethyl)aminomethane (Tris), DL-methionine, and riboflavin were purchased from Energy Chemical (China). Nitro blue tetrazolium and 2,2-diphenyl-1-picrylhydrazyl (DPPH) were obtained from TCI Chem Shanghai (China). Anhydrous ethanol, methanol, acetic acid (HAc), and other solvents were obtained from Damao Chemical Reagent Factory (Tianjin, China). Prothrombin time (PT) and activated partial thromboplastin time (APTT) kits were purchased from Qingdao Heall Bio-science Technology Co., Ltd (China). Absorbable gelatin sponge (GS) was purchased from Jinling Pharmaceutical Co., Ltd (China). The strain of *Staphylococcus aureus* (*S. aureus*, CMCC (B) 26003) was a gift from Prof. Xing Wang, Beijing University of Chemical Technology (China).

2.2. Preparation of CGS

Chitosan was dissolved into a mixture solution of HAc and deionized (DI) water solution (v/v, 1/149) under magnetic stirring at room temperature (RT) to produce solution A (26 mg mL^{-1}). Gelatin was dissolved in DI water under magnetic stirring at 37 °C to produce solution B (26 mg mL^{-1}). Different amounts of solution A and solution B (at the mass ratios of 7/3, 5/5, 3/7) were mixed under low-speed mechanical stirring (300 rpm, 15 min; using an electric mixer equipped with an egg whisk), and then stirred vigorously (1000 rpm, 30 min) to form foaming solutions. Thereafter, the obtained foaming solutions were poured in watch glasses, frozen quickly at −80 °C, and lyophilized to produce crude sponges. Finally, the crude sponges were washed with anhydrous ethanol and vacuum dried to produce the CGS samples. Based on the different mass ratios of solution A/solution B (7/3, 5/5, and 3/7 a), the corresponding CGS7, CGS5, and CGS3 samples were prepared. Also, single solution A or solution B was also used to prepare chitosan or gelatin sponge adopting the aforementioned procedures, and these samples were named as CGS10 or CGS0.

2.3. Preparation of PCGS

The Tris–HCl aqueous solution (1 mg mL^{-1}, pH 8.5) was first prepared and used to mix with anhydrous ethanol (v/v, 9/1), producing Tris/ethanol solution. PC was dissolved in Tris/ethanol solution to prepare PC solution at a concentration of 3 mg mL^{-1}. Thereafter, the prepared CGS7 (or CGS10) was cut into small pieces (with each piece normally weighing 20 mg), soaked into PC solution (normally 4 mL per piece) for 10 min, and washed with DI water three times (to remove residual PC). Finally, the obtained crude sponge pieces were frozen at −80 °C and lyophilized to produce PCGS7 (or PCGS10). Notably, the PC solution at 1 mg mL^{-1} (or 5 mg mL^{-1}) and pure Tris/ethanol solution were also used for the post-treatment of CGS7 and CGS10 adopting the aforementioned procedures, to produce CGS7 & PC (1, 5, or 0 mg mL^{-1}) and CGS10 & PC (1, 5, or 0 mg mL^{-1}).

2.4. Physical characterization

To observe the interior morphologies of CGS and PCGS sponges,[12] the sponges were rapidly quenched in liquid nitrogen, carefully cut into two pieces, and the sponges were fixed onto an appropriative platform by conductive tapes and coated with platinum, prior to visualizing their cross-sections by scanning electron microscopy (SEM; JEOL, JSM-7500F, Japan). To calculate the carbon (C)/hydrogen (H)/nitrogen (N) contents of the CGS and PCGS samples, the sponges were dried in an air oven and weighed to obtain 2 mg of sample, prior to analyzing their element contents under a helium atmosphere using an Elemental analyzer (Elementar, Vario ELcube, Germany). To measure the surface charges of the CGS and PCGS samples,[22] the sponges were cut into ultrasmall particles, filtered through a metallic sieve (50 mesh, to remove big particles) and dispersed in DI water (2 mg mL^{-1}) under sonication, prior to analyzing the zeta potentials of the sponge particles by dynamic light scattering (DLS, Malvern, Zetasizer Nano ZS, UK).

To measure the liquid-absorption capacity of the CGS and PCGS samples, a small piece of sponge was pre-weighed as m_0, soaked into a watch glass filled with abundant liquid (DI water, normal saline, or citrated whole blood extracted from Sprague–Dawley (SD) rats), and weighed as m_1 after saturated absorption (using a tweezer to take out and hover the sponge for 30 s in air in advance, to ensure the equilibrium of liquid absorption). The swelling ratio (SR, %) of the sponges was calculated from eqn (1) and the photographs of the sponges before and after water absorption were also captured,

$$\mathrm{SR}(\%) = \frac{m_1 - m_0}{m_0} \times 100\%. \quad (1)$$

Notably, whole blood was drawn from the heart of healthy Sprague–Dawley (SD) rats (male, 200–300 g, obtained from Beijing Vital River Laboratory Animal Technology Co., Ltd, China) and immediately stored in anticoagulant tube (containing sodium citrate), which was named as citrated whole blood and also used in the following hemolysis and in the *in vitro* hemostatic assays. All the animal procedures were performed in accordance with the rules of the Institute of Clinical Medicine, China-Japan Friendship Hospital (Beijing, China).

2.5. Hemolysis assay

The hemolysis rates of the CGS and PCGS samples were assessed by the standard procedures of hemolysis assay, which

was described in our previous work.[10,12] Key parameters were provided as follows: (1) red blood cell (RBC) suspension (at a volume concentration of 2%) was prepared from citrated whole blood and dispersed in phosphate buffered saline (PBS); (2) 2 mg (or 5 mg) of sponge was added with 1 mL of RBC suspension (to achieve a concentration of 2 or 5 mg mL^{-1}) and incubated at 37 °C for 3 h; (3) cell lysate (Trition X-100, at a volume of 2% in DI water) and PBS were set as the positive and negative control groups, respectively.

2.6. *In vitro* hemostatic assays

The blood clotting index (BCI) assays of the CGS and PCGS samples were performed as follows: first, the sponges were cut into small pieces (2 mg), each of which was placed in a plastic centrifuge tube (incubated at 37 °C in a water bath) and used the same way in the following PT and APTT assays. Second, 100 μL of citrated whole blood was added to the sponge pieces, and immediately 10 μL of $CaCl_2$ aqueous solution (0.2 M) was added followed by incubation at 37 °C for 5 min. Third, the BCI value (%) of the sponge pieces was measured by quantifying the percentage of RBCs not involved in the blood clots, adopting the same procedures in our previous work.[23] Notably, the BCI values of CGS7 & PC (1, 5, or 0 mg mL^{-1}) and CGS10 & PC (1, 5, or 0 mg mL^{-1}) were also measured adopting the aforementioned procedures.

The PT and APTT values of the CGS and PCGS samples were assessed by the standard procedures as described in our previous work.[23] Key parameters were provided as follows: (1) citrated whole blood was centrifuged (3000 rpm, 15 min) to carefully collect the supernatant as platelet-poor plasma (PPP); (2) 2 mg of each sponge piece (in a plastic centrifuge tube, at 37 °C in a water bath) was added to 100 μL of PPP and PT (or APTT reagent) to measure the PT (or APTT) values; (3) the PT and APTT values of 100 μL of PPP were also measured and used as the blank group (untreated blood).

2.7. Free-radical scavenging assays

The DPPH scavenging assays of the CGS and PCGS samples were assessed as follows.[24] First, the sponges were cut into ultrasmall particles and dispersed into DPPH methanol solution (0.1 mM) at the concentration of 2 mg mL^{-1}. The blank control group was the DPPH methanol solution alone. Second, all the samples were incubated in a completely dark environment for 30 min. Third, the absorbance of each sample was measured at 517 nm and the DPPH scavenging efficiency (%) was calculated from eqn (2),

$$\text{DPPH scavenging efficiency}(\%) = \frac{A_B - A_S}{A_B} \times 100\%, \quad (2)$$

where A_B and A_S were the OD values of the blank and sample groups, respectively.

The superoxide radical ($O_2^{\bullet-}$) scavenging assay of the CGS and PCGS samples were assessed as follows.[25] First, the $O_2^{\bullet-}$ working solution was prepared by dissolving riboflavin (20 μM), DL-methionine (12.5 mM), and nitro blue tetrazolium (75 μM) into PBS solution (25 mM, pH 7.4) in a completely dark environment. Second, the sponges were cut into ultrasmall particles and dispersed into the aforementioned working solution at the concentration of 2 mg mL^{-1}. The blank control group was the working solution alone. Third, all the samples were incubated upon ultraviolet irradiation for 15 min. Finally, the absorbance of each sample was measured at 560 nm and the $O_2^{\bullet-}$ scavenging efficiency (%) was calculated from eqn (3),

$$O_2^{\bullet-}\text{ scavenging efficiency}(\%) = 1 - \frac{A_S - A_0}{A_B - A_0} \times 100\% \quad (3)$$

where A_S and A_B are the OD values of the sample and blank groups after irradiation, and A_0 is the OD value of the blank group before irradiation.

2.8. *In vitro* antibacterial assay

The antibacterial activity of PCGS against *S. aureus* was assessed by the similar procedures described in our previous work[23] (with slight modifications, due to the insolubility of the sponges in aqueous medium). First, the sponges were first cut into ultrasmall particles and weighed to obtain 1–6 mg of samples. Each sponge sample was placed in one sterilized centrifuge tube and sterilized by ultraviolet light irradiation. Second, based on the optical density (at 600 nm, OD600) of the bacterial suspension in LB medium (*i.e.*, a bacterial suspension with an OD of 0.8 indicates the concentration of 0.8×10^8 CFU mL^{-1}), the cultured bacterial suspension was diluted to 1×10^5 CFU mL^{-1} by LB medium. Next, 1 mL of diluted bacterial suspension was added with the sponge sample (to achieve the final concentrations from 1–6 mg mL^{-1}), prior to incubation at 37 °C for 12 h by a constant temperature shaker. Also, 1 mL of diluted bacterial suspension was incubated in one sterilized centrifuge tube (at 37 °C for 12 h) and used as the blank group (untreated bacteria). Third, the surviving bacteria in the sponge and LB medium were washed with sterilized PBS, the volume of which was fixed as 1 mL. Next, 100 μL of bacterial suspension of the sponge-treated or blank group (diluted by PBS by 10, 100, 1000, or 10 000 times for better colony counts) was spread evenly on an agar plate/medium, incubated at 37 °C for 24 h and finally photographed for obtaining the colony count. Finally, the bacterial inhibition efficiency (η) was calculated from eqn (4),

$$\eta(\%) = \frac{N_B - N_S}{N_B} \times 100\%, \quad (4)$$

where N_B and N_S are the number of bacteria (determined by colony count) in the blank and sample groups after 12 h of incubation. Notably, the minimum inhibitory concentration (MIC) of sponges was defined as the minimum inhibitory concentration for $\eta > 99.9\%$.

2.9. *In vivo* hemostatic assay of PCGS

The *in vivo* femoral-artery-injury model was performed on SD rats (male, 180–210 g), which was according to our previous paper.[23] All the animal procedures were performed in accordance with the rules of the Institute of Clinical Medicine,

China-Japan Friendship Hospital (Beijing, China) and all the experimental protocols were approved by the Animal Ethics Committee of China-Japan Friendship Hospital (grant no. 190101). Key procedures were provided as follows: (1) the rats were randomly divided into three groups: (1) PCGS7 group treated with dry PCGS7 (1.5 × 1.5 cm), (2) GS-dry group treated with dry GS (1.5 × 1.5 cm), and (3) GS-wet group treated with wet GS (moistened by normal saline in advance, 1.5 × 1.5 cm); (2) the femoral artery and surrounding vein and nerve were cut off with a scalpel together to create the femoral-artery-injury model, since the latter two were difficult to be separated from the artery; (3) the cut-off femoral artery of each group was allowed to freely bleed for 10 s prior to applying the sponge, with the blood loss collected counted among the pre-treatment blood loss. Only rat samples with s pre-treatment blood loss of 180–360 mg were selected for the final analysis of the post-treatment blood loss and hemostatic time, to reduce the influence of individual differences of the rats and operation error among the three groups; *i.e.*, PCGS7 group, n = 5; GS-dry group, n = 3; GS-wet group, n = 3.

2.10. *In vivo* infected wound-healing assay of PCGS

The *in vivo* infected-tooth-extraction model was performed on SD rats (male, 130–190 g). All the animal procedures were performed in accordance with the rules of the Institute of Dental Research, Capital Medical University (Beijing, China) and all the experimental protocols were approved by the Animal Ethics Committee of Capital Medical University (grant no. KQYY-201610-001). Detailed procedures were provided as follows: (1) *S. aureus* suspensions containing 10^9 CFU were centrifuged to get the bacterial sediment and were stored in 1.5 mL centrifuge tubes (10^9 CFU per rat in the infected groups). Next, 1 mL of adrenaline hydrochloride injection (1 mL : 1 mg, obtained from Tianjin Kingyork Pharmaceutical Co., Ltd, China) was diluted with 9 mL of normal saline to get the working solution for adrenaline treatment. The PCGS7 sample was cut into ultrasmall particles and sterilized by ultraviolet light irradiation; (2) during tooth extraction and filling the sockets, the mice were anesthetized by the intraperitoneal injection of chloral hydrate (10% in DI water, 0.3 mL per 100 g weight); (3) after the disconnection of the surrounding gingiva without root fracture or bone cataclasis, the right incisor of the upper jaw was gently extracted using forceps. Upon such tooth extraction (day 0), the sockets of the rats received different treatments in the four groups: the soft tissues of tooth-extraction sockets were immediately sutured with absorbable surgical sutures (Mersilk 5-0, W580, Ethicon, USA) in the control group; the sockets were treated with medical cotton balls (Qingdao Hainuo Biological Engineering Co., Ltd, China) for 2–4 min (to avoid continuous blood loss), immediately filled with bacterial sediment (cotton balls was removed, not implanted in the sockets) before suturing soft tissues in the INF group; the sockets were treated with adrenaline hydrochloride working solution (loaded in medical cotton balls) for 1–2 min to achieve complete hemostasis (a clean socket with few blood clots, due to the rapid hemostasis), immediately filled with bacterial sediment, and finally sutured in the ADR group; the sockets were treated with PCGS7 for 1–2 min to achieve complete hemostasis, filled with bacterial sediment, and finally sutured in the PCGS7 group; (4) in order to evaluate the healing process, half of the rats were euthanized on days 7 (n_1 = 3 or 4) and 14 (n_2 = 3 or 4) to harvest the maxilla.

The harvested maxilla samples were captured and handled as follows, prior to histological evaluation.[26] First, the maxilla samples were fixed in neutral buffered formalin (10%, RNase free, Beijing Solarbio Science & Technology, China) for 48 h. Second, each sample was cut into two pieces through the middle of socket and along the sagittal plane of the socket by a low-speed saw, to expose the inner side of the tooth socket prior to decalcification. The samples were then demineralized in ethylenediaminetetraacetic acid solution (10%) for 2 weeks. Third, the samples were dehydrated by gradient ethanol (75%, 85%, 90%, 95%, and 100%), treated with a mixture of ethybenzene and xylene, and embedded in paraffin. Finally, the slices of the samples (4 μm in thickness) were prepared by a microtome (RM2016, Leica, Germany) and stained with hematoxylin and eosin (H&E). The area ratio of the inflammatory cells and sponge particles within the sockets were observed by an optical microscope and calculated using Image J software (National Institutes of Health version 2.0). The area ratio of inflammatory cells and of the sponge particles were standardized by the areas of the local section and tooth socket, respectively.

2.11. Statistical analysis

All the experiments were repeated at least three times for statistical analysis and the data were presented as the means ± standard deviation. One-way ANOVA with Bonferroni's correction was used to compare differences between at least three groups, and Student's t test for two groups. In all the pictures, $p^* < 0.05$ represents one asterisk, $p^{**} < 0.01$ represents two asterisks, $p^{***} < 0.001$ represents three asterisks.

3. Results and discussion

3.1. Preparation and characterization of the CGS

The preparation process of the CGS is illustrated in Fig. 1. First, chitosan and gelatin were mixed in the aqueous phase and stirred vigorously using an egg whisk. The mixture solutions of CGS7, CGS5, and CGS3, as well as the gelatin solution of CGS10, could generate foaming solutions under such vigorous stirring (Fig. S1†). On the contrary, the chitosan solution of CGS10 did not become highly foaming after vigorous stirring due to the absence of amphiphilic gelatin. Such a phenomenon could be attributed to the findings in our previous work that the amphiphilic component, a highly viscous solution, and vigorous stirring are the critical factors for self-foaming aqueous solutions.[12] Since no extra foaming agent was required, the self-foaming process of the CGS samples was performed under a facile 'green' condition, which is favorable for scale production. Second, the foaming solution was lyophi-

lized and completely dried by ethanol treatment to produce the CGS (Fig. 1). As shown in Fig. 2a, the interior morphologies of the different CGS samples were observed by SEM. CGS10 displayed a typical lamellar structure after the lyophilization of the highly hydrophilic chitosan alone (in HAc solution), while CGS0 presented a three-dimensional network and highly porous morphology after the lyophilization of the foaming gelatin solution. Moreover, CGS7, CGS5, and CGS3 exhibited the combined morphology of the lamellar CGS10 and three-dimensional porous CGS0, which was in accordance with their composite components of chitosan and gelatin.

Hemostatic sponges have been commonly designed for absorbing blood quickly and for concentrating blood components (*i.e.*, platelets and RBCs) to accelerate hemostasis.[12–14] Thus, the liquid-absorption capacity of the CGS samples was tested as a critical indicator for potential hemostatic uses. Fig. 2b–d display the swelling ratios of the CGS samples in three different liquids (DI water, normal saline, or whole blood). CGS0, despite its highly porous structure, exhibited the lowest swelling ratio (~4 in all three liquids) among all the five sponges. In comparison, CGS10 achieved obviously higher swelling ratios (~40 for DI water, and ~27 for normal saline and whole blood). Such a distinct liquid-absorption capacity of CGS10 and CGS0 could be attributed to the structure difference between chitosan and gelatin chains. The chitosan chains in CGS10 could produce moderate physical cross-linking sites *via* hydrogen bonds and hydrophobic interactions —enhanced by the ethanol treatment (removing residual HAc) after lyophilization—which contributed to it absorbing a lot of liquid among the whole sponge. Due to the lack of chemical cross-linking agents (*i.e.*, glutaraldehyde used for clinical GS), the interactions between amphiphilic gelatin chains probably

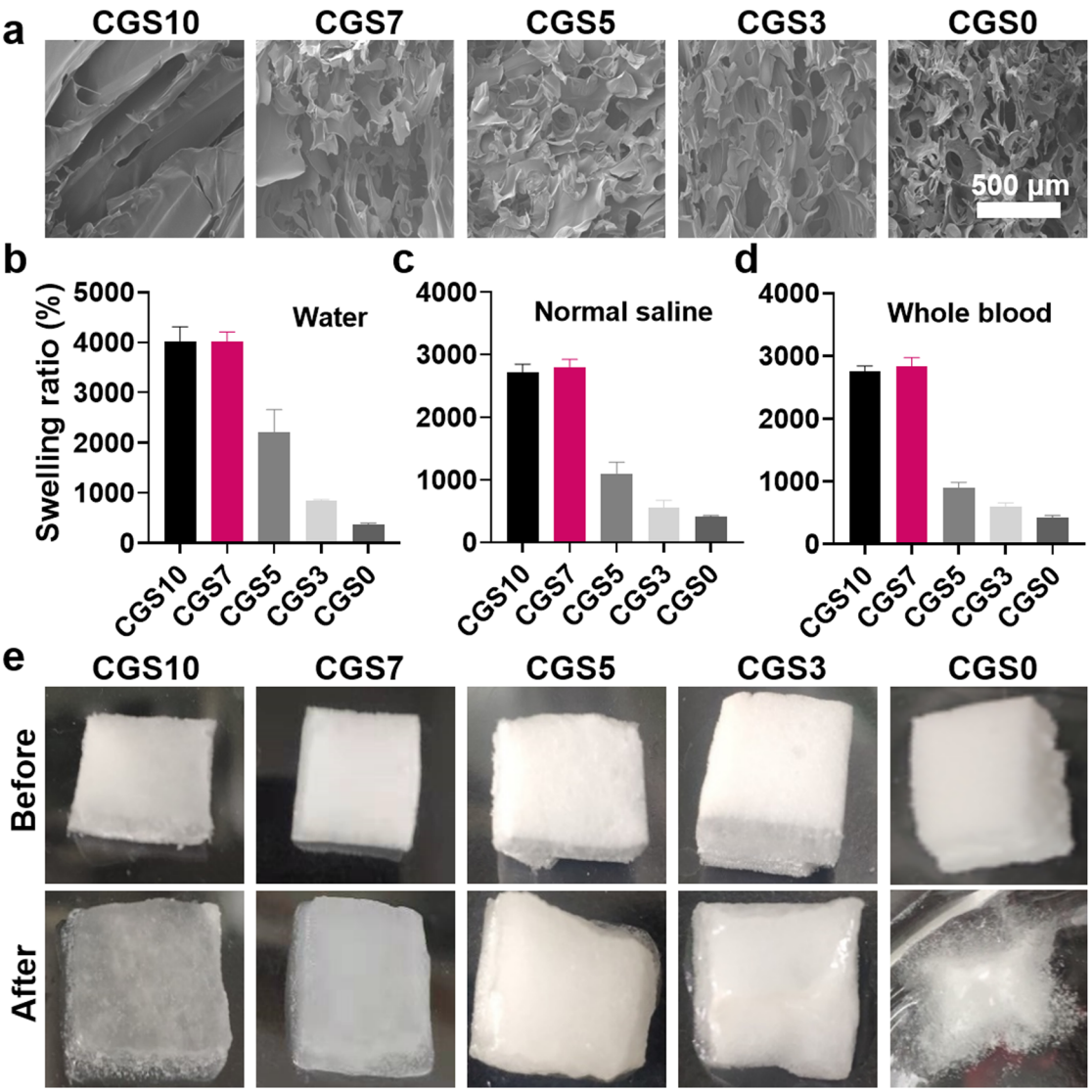

Fig. 2 (a) SEM image of the interior morphology, (b–d) swelling ratios in water/normal saline/whole blood (mean ± SD, n = 3), and (e) photographs before and after water absorption of the CGS.

could not afford the necessary cross-linking sites/strength for its three-dimensional network, thus hindering the subsequent liquid absorption, which was probably worsened by the highly porous morphology of CGS0. Fig. 2e shows the photographs of the CGS samples before and after the saturated absorption of DI water, which further supports the aforementioned explanations. CGS10 exhibited a sufficient absorption of water, with an obvious volume expansion while maintaining its original shape, confirming its moderate cross-linking state. On the contrary, CGS0 broke up after swelling and merely absorbed water on the surface.

Interestingly, the swelling ratios of CGS3, CGS5, and CGS7 increased obviously with the decrease in gelatin content, which revealed that both their interior morphology and liquid-absorption capacity presented the combined effects from pure gelatin and chitosan sponges (Fig. 2b–d). Specially, CGS7 exhibited high swelling ratios in the three liquids (similar to CGS10), which may be due to the good balance between the moderate physical cross-linking sites (endowed by chitosan) and highly porous morphology (endowed by the gelatin-induced self-foaming process). All the above results demonstrated the high liquid-absorption performance of CGS10 and CGS7. Meanwhile, the *in vitro* BCI assay further confirmed that CGS7 possessed the best *in vitro* hemostatic property among the five CGS samples (Fig. S2†). Thus, CGS7 was selected for the subsequent construction of PC-functionalized biomedical sponges, with CGS10 was used for the control group.

3.2. Preparation and characterization of PCGS

Naturally occurring polyphenols have received great attention in the biomedical field, due to their favorable antimicrobial and antioxidant property for wound healing.[27,28] Owing to the efficient Schiff base reaction of phenolic hydroxyls and amino groups (of chitosan/gelatin),[29] PC was incorporated in to CGS samples to optimize their applications for hemostasis and wound healing. The selected CGS7 and CGS10 were immersed into 3 mg mL^{-1} of PC solution and lyophilized to facilely produce the corresponding PCGS7 and PCGS10. To note, the Tris/ethanol solution for dissolving PC, consisting of Tris–HCl aqueous solution and ethanol (v/v, 9/1), was elaborately designed for such secondary (chemical) cross-linking reaction of the CGS in this work. The abundant alkaline Tris–HCl aqueous solution could facilitate the cross-linking reaction. More importantly, the indispensable ethanol—as a participant or poor solvent of CGS—could effectively decrease their volume expansion upon the initial adsorption of Tris–HCl aqueous solution and ensure the shape stability for the second lyophilization.

As shown in Fig. 3a, both PCGS7 and PCGS10 displayed a uniform reddish brown appearance before and after the absorption of DI water, which was different from the white CGS samples. As shown in Fig. 3b, the zeta potentials of PCGS7 and PCGS10 (determined from the sponge particle size by DLS) were decreased obviously in comparison with those of CGS7 (18 ± 3.33 mV *vs.* 5 ± 1.55 mV) and PCGS 10 (8.74 ± 1.55 mV *vs.* 5.87 ± 0.82 mV), due to the consumption of amino groups and the incorporation of phenolic hydroxyls. The elemental analysis results further confirmed the existence of PC on the PCGS samples (Fig. 3c). Owing to the introduction of nitrogen-free PC, PCGS7 and PCGS10 possessed lower N/C ratios than the corresponding CGS7 and CGS10. The PC contents of PCGS7 and PCGS10 were calculated to be 81.7 and 81.8 mg g^{-1}, respectively (Table S1†). Meanwhile, the SEM images in Fig. 3d show that PCGS7 (or PCGS10) exhibited a highly similar interior morphology with the original CGS7 (or CGS10), indicating the mild/uniform cross-linking process of the PC and CGSs in Tris/ethanol solution. All these results demonstrated that PC could be well incorporated in CGSs to produce PCGSs, using a facile solution-soaking process.

Specially, the secondary cross-linking of PC played a different role on the liquid-absorption capacities of PCGS7 and PCGS10 (Fig. 3e), despite their similar appearance and PC content. Compared with the original CGS10, PCGS10 had almost unchanged swelling ratios in the three liquids. On the contrary, the swelling ratios of PCGS7 were obviously higher than those of CGS7, especially for normal saline and whole blood (~40 *vs.* ~30). Both moderate cross-linking sites and the interior porous structure were revealed to be crucial for a high liquid-absorption capacity of sponges.[12] It can be inferred that the incorporation of PC probably generated a compromised effect on the total cross-linking state of PCGS10, which would endow some chemical cross-linking sites but simultaneously weaken the physical cross-linking state (by decreasing the regularity and hydrophobicity) of the chitosan chains, resulting in no improvement in the liquid-absorption capacity. Apart from the similar compromised effect on chitosan chains, PC would endow appropriate chemical cross-linking sites for the gelatin chains and effectively strengthen the highly porous interior morphology of CGS7. In other words, compared with CGS7, PCGS7 with incorporated PC could achieve more suitable/higher cross-linking sites for a highly porous morphology (endowed by the self-foaming gelatin) to further improve the liquid-absorption capacity.

3.3. *In vitro* hemostatic assays of PCGS

As a prerequisite for potential biomedical dressings, the hemolysis assay was performed on the CGS and PCGS samples to evaluate their blood compatibility.[30] Chitosan-based CGS10 exhibited a low hemolysis rate of ~3% at the concentration of 2 mg mL^{-1} (Fig. 4a and Fig. S3†), while its hemolysis rate increased to >5% at a higher concentration of 5 mg mL^{-1}. In contrast, CGS7 and PCGS7 exhibited lower, qualified hemolysis rates (<5%) at both 2 and 5 mg mL^{-1}. The high cationic charges of chitosan, as indicated by the high zeta potential of CGS10 (Fig. 3b), would probably have a harmful effect on RBCs and could be weakened by the incorporated gelatin.

To investigate the role of PC cross-linking on the hemostatic property of the sponges, the BCI and PT/APTT assays were performed on CGS and PCGS samples. As shown in Fig. 4b, PCGS7 exhibited lower BCI values than the corresponding CGS7&PC0 (which refers to CGS samples treated with Tris/ethanol solution without PC), indicating the enhanced hemo-

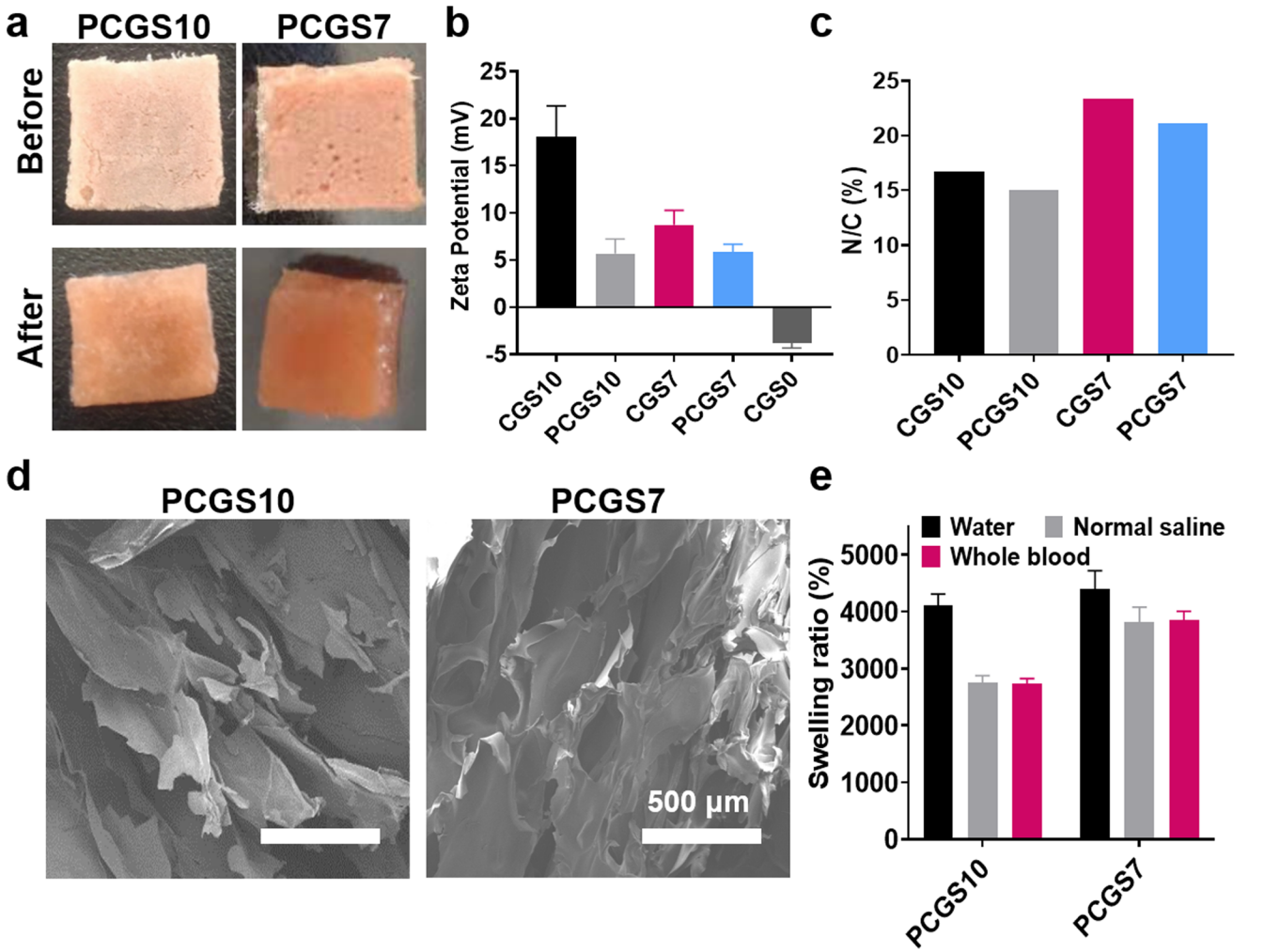

Fig. 3 (a) Photographs before and after water absorption, (b) zeta potential of the corresponding sponge particles (mean ± SD, n = 5), (c) element content (N/C ratio), (d) SEM image of the interior morphology, and (e) swelling ratios in water/normal saline/whole blood (mean ± SD, n = 3) of the PCGS.

static property through the PC cross-linking process. PT's results revealed the normal exogenous coagulation system of the CGS- or PCGS-treated plasma (Fig. 4c), as indicated by their similar PT values to the blank group (untreated plasma). Meanwhile, the endogenous coagulation system of plasma was highly suppressed after the incubation with CGS7&PC0 and CGS10&PC0 (Fig. 4d, APTT values greater than 2-fold that of the blank group), while the PCGS7 and PCGS10 groups exhibited the normal endogenous coagulation system. Thus, the interference of the chitosan component with several anionic clotting factors (involving the endogenous coagulation system) was effectively alleviated by the incorporation of PC, accompanied by a decrease in the surface charges (Fig. 3b), which was inferred to be the key mechanism for the enhanced hemostatic property of PCGS7. Moreover, the BCI value of PCGS7 was significantly lower than that of PCGS10. Considering their similar PT/APTT values, the higher hemostatic property of PCGS7 (over PCGS10) could be attributed to the higher blood-absorption capacity of PCGS7 (as shown in Fig. 3e) and the resultant more efficient blood absorption and blood component concentration. In addition, the BCI assay further revealed that the optimal PC concentration for hemostasis was the adopted 3 mg mL^{-1} for PCGS7, which displayed the lower BCI values of PCGS7 than for CGS7&PC1 or CGS7&PC5 (Fig. S4†).

3.4. Antioxidant and *in vitro* antibacterial assays of PCGS

Owing to the reported antioxidant property of polyphenols,[27] the DPPH and superoxide radical scavenging assays were performed on the CGS and PCGS samples to investigate their antioxidant property. As shown in Fig. 5a, CGS7 and CGS10 displayed negligible DPPH scavenging efficiency, while PCGS7 and PCGS10 exhibited the expected higher DPPH scavenging efficiencies due to the incorporation of PC. In addition, PCGS7 and PCGS10 possessed favorable scavenging efficiencies toward superoxide radicals (Fig. 5b). It has been reported that biomedical materials with antioxidant property would be valuable for treating chronic wounds,[24,25] as they can alleviate/

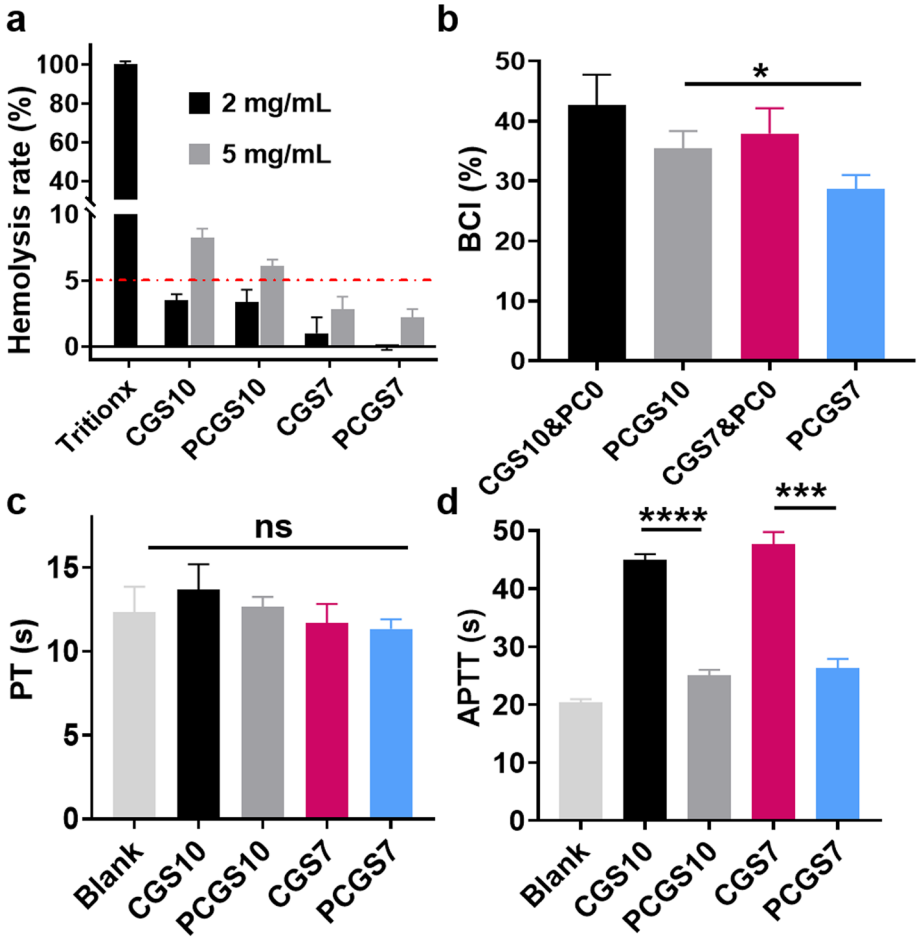

Fig. 4 (a) Hemolysis rate (mean ± SD, n = 3), (b) BCI value (mean ± SD, n = 3, *p < 0.05, Student's t test), (c) PT value (mean ± SD, n = 3, not significant (ns) p > 0.05, one-way ANOVA), and (d) APTT value (mean ± SD, n = 3, ***p < 0.001, ****p < 0.0001, Student's t test) of the CGS and PCGS.

shorten the inflammation response and accelerate wound healing. Therefore, such a good antioxidant property of PCGS would probably benefit the wound-healing process after successful hemostasis.

Considering the antibacterial ability of the individual chitosan and polyphenols,[27] the MIC assay was performed on CGS and PCGS samples *to* evaluate their *in vitro* antibacterial ability. Notably, the bacterial numbers of the sponge-treated/sample groups and blank groups were determined by bacterial colony counting (after spreading on agar plates), due to the inconvenience/possible errors in optical density measurements from the mixtures of bacterial suspensions and opaque sponges. As shown in Fig. 5c and Fig. S5,† the MICs for CGS10 and CGS7 toward *S. aureus* were 4 and 2 mg mL^{-1}, respectively. On the one hand, such MIC results confirmed the antibacterial ability endowed by chitosan, the mechanism of which involved the electrostatic interaction of cationic chitosan chains with the negatively charged cytoplasmic membrane and a subsequent inhibition of membrane transport.[31–33] On the other hand, the lower MIC of CGS7 than CGS10 indicated the higher antibacterial ability of CGS7, despite the former being composed of a lower content of chitosan. Compared with lamellar CGS10, three-dimensional porous CGS7 probably generated a better interaction of chitosan chains with *S. aureus*, benefiting the antibacterial ability. Specifically, after the incorporation of PC, both PCGS7 and PCGS10 exhibited the same MIC of 6 mg mL^{-1} (higher than the original CGS), which indicated the negative effect of PC on the antibacterial ability of the PCGSs. Such a phenomenon could be explained as follows: (1) the incorporated PC was covalently grafted with chitosan or gelatin chains, which was difficult to dissociate (from the PCGS) into the bacterial suspension. Unlike free polyphenols that can transport into bacterial cells and induce metabolic disorder,[34] such an immobilized PC would probably fail to inhibit the bacterial growth; (2) after the incorporation of PC, the decreased surface charges probably weakened the interaction of the PCGSs (chitosan chains) with *S. aureus* and reduced the antibacterial ability. To sum up, all the results demonstrated that PCGS7 achieved a medium antibacterial ability against *S. aureus* but promising antioxidant and *in vitro* hemostatic properties. Taking the facile preparation procedures and the total biomass-derived ingredients (gelatin, chitosan, and polyphenol) into account, such multifunctional PCGS7 has high potential for clinical uses as a wound dressing

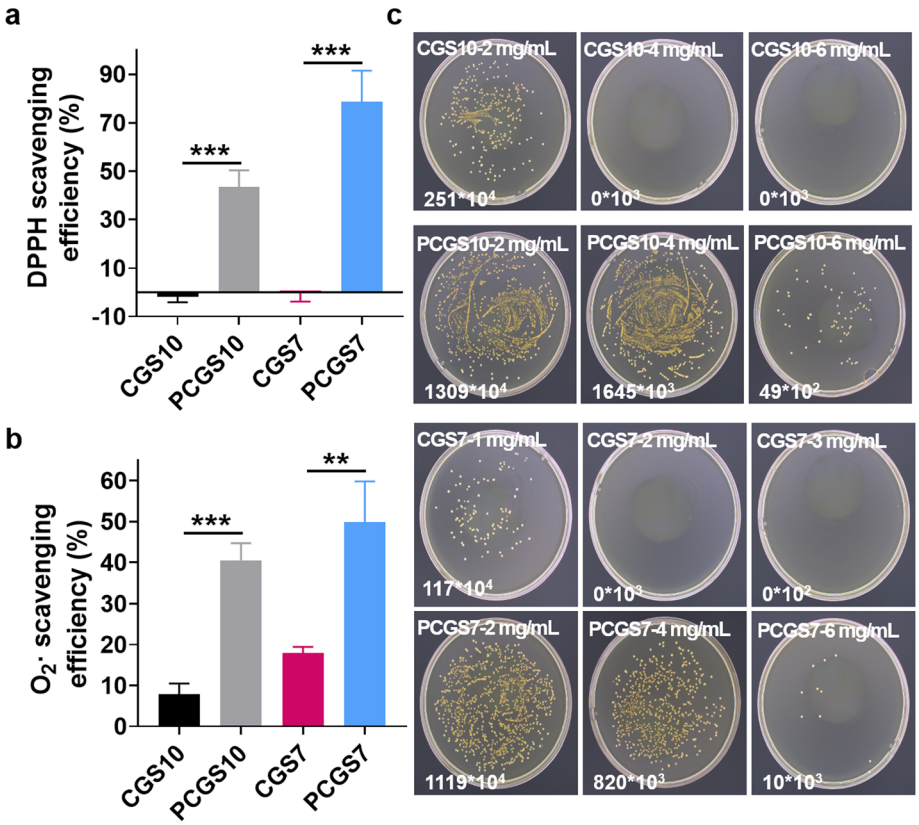

Fig. 5 (a and b) Scavenging efficiency of DPPH and superoxide radicals (mean ± SD, $n = 3$, $^{**}p < 0.01$, $^{***}p < 0.001$, Student's t test), and (c) photographs of bacterial cultures in the PCGS and CGS groups (the colony number * dilution ratio in the inserts).

and was thus further investigated in the following *in vivo* study.

3.5. *In vivo* hemostatic assay of PCGS

A femoral-artery-injury model was first established to evaluate the *in vivo* hemostatic performance of PCGS7 in SD rats (Fig. 6a). Commercial GS was chosen for two control groups: according to the supplier's instructions, GS-dry and GS-wet groups were adopted based on applying the dry and wet GS (moistened by normal saline in advance) for hemostasis, respectively. To minimize individual difference/operation errors, the pre-treatment blood loss (free bleeding for 10 s before applying the sponges) of each group was measured and the results are shown in Fig. 6b. After selecting 180–360 mg for the qualified samples, there was no significant difference among the amounts of pre-treatment blood loss of the three groups. On this basis, the post-treatment blood loss could reflect the hemostatic performance of three groups. As shown in Fig. 6c, the PCGS7 group exhibited a significantly lower amount of blood loss than the GS-dry and GS-wet groups. Meanwhile, the different blood losses were also visualized by photographs of the three sponges after hemostasis, which further supported the lowest amount of absorbed blood on PCGS7. Notably, reducing blood loss is commonly recognized as the primary property of hemostatic materials/devices, as the amount of blood loss is crucial to the body's health (or even mortality) after intractable or severe bleeding.[23,35] Due to such obviously reduced blood loss compared to commercial sponges/devices, PCGS7 has great potential for clinical hemostasis utility.

3.6. *In vivo* wound-healing assay of PCGS

Tooth-extraction bleeding is a frequent but unique wound scenario after tooth extraction, which calls for wound dressings not limited to single hemostasis. For instance, adrenaline is usually applied to stop tooth socket bleeding in clinic treatment, but adrenaline-induced excessive (too rapid) hemostasis may increase the risk of infection and generate "dry socket".[18] Therefore, the *in vivo* infected-tooth-extraction model (which corresponds to the clinical scenario of oral bacterial infection after tooth extraction) was further performed on SD rats to evaluate the effect of PCGS7 on anti-infection and wound healing. The rats were randomly divided into four groups (each n = 6–8) and received different treatments: control group (without hemostatic agent, without bacterial infection), INF group (without hemostatic agent, with bacterial infection), ADR group (with clinical adrenaline treatment for hemostasis and bacterial infection), and PCGS7 group (with PCGS7 treatment for hemostasis and bacterial infection). Fig. 7a displays representative photographs of harvested maxilla samples on days 7 and 14, which can be used to

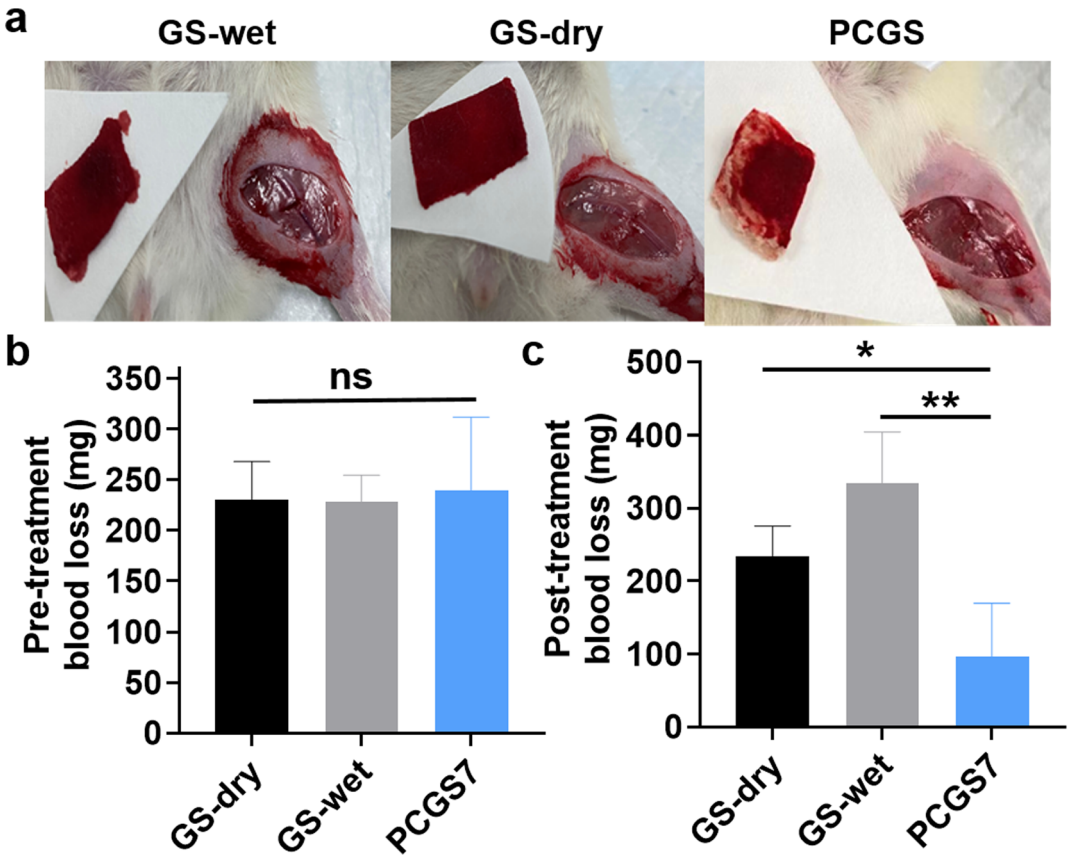

Fig. 6 *In vivo* hemostatic performance of PCGS7 in the rat femoral-artery-injury model: (a) representative photographs and (b and c) pre-/post-treatment blood loss (mean ± SD, $n \geq 3$, not significant (ns) $p > 0.05$, *$p < 0.05$, **$p < 0.01$, one-way ANOVA) in the GS-dry, GS-wet, and PCGS7 groups.

observe the general view of tooth extraction sockets. As for the control group, the gingiva of the extraction socket was completely closed from day 7, accompanied with a normal color and flat appearance, representing an ideal/undisturbed healing process for uninfected tooth-extraction sockets.[26,36] However for the ADR group, the soft tissues at the tooth-extraction socket were severely swollen/cracked and the bone surface was highly exposed on day 7 (as indicated by the dashed green circle), revealing the worst healing state among the four groups and the expected delay of wound healing by the excessive hemostasis of clinical adrenaline treatment. By comparison, the PCGS7 group displayed the closed gingiva and unexposed bone surface on day 7 (as indicated by the green arrow), but the gingiva of the extraction socket was uneven, pitted, or gaped. On day 14, the ADR group maintained the worst healing state, as indicated by the exposed bone tissue and not completely closed gingiva, while the PCGS7 group displayed the further improved gingiva (*i.e.*, the gaps became smaller than those on day 7). The general view of the results clearly revealed that PCGS7 treatment could achieve better healing quality than clinical adrenaline treatment in the infected-tooth-extraction model, probably due to the multi-functions of PCGS7 (including antibacterial and antioxidant properties, but not limited to simple hemostasis).

Specially, the INF group exhibited the unexpected good healing state of the extraction socket on day 14 (Fig. 7a), which was similar to in the PCGS7 group. Hence, histological section analysis was further adopted to evaluate the healing process of the extraction sockets in the four groups. Hematoxylin and eosin (H&E) analysis revealed the distinct cell/tissue responses of the four groups on days 7 and 14 (Fig. 7b and Fig. S6†). On day 7, the INF and ADR groups exhibited a large number of inflammatory cells (indicated by white arrows) had filtrated into the extraction socket, and even a pyocyte mass (indicated by red pentagrams). On the contrary, sponge particles (indicated by yellow pentagrams) were observed to have filled in the extraction sockets in the PCGS7 group, while only a small amount of inflammatory cells had infiltrated around the material. The quantitative analysis further confirmed that the relative area of inflammatory cells in the PCGS7 group was significantly lower than those of the INF and ADR groups on day 7 (Fig. 7c), which could be attributed to the combination of antibacterial and antioxidant properties of PCGS7. On day 14, a pyocyte mass and large number of inflammatory cells were still observed in the extraction socket of the ADR group (Fig. 7b), which was consistent with the worst healing state of the ADR group (Fig. 7a) after such a severe inflammatory response. On the contrary, both the PCGS7 and INF groups

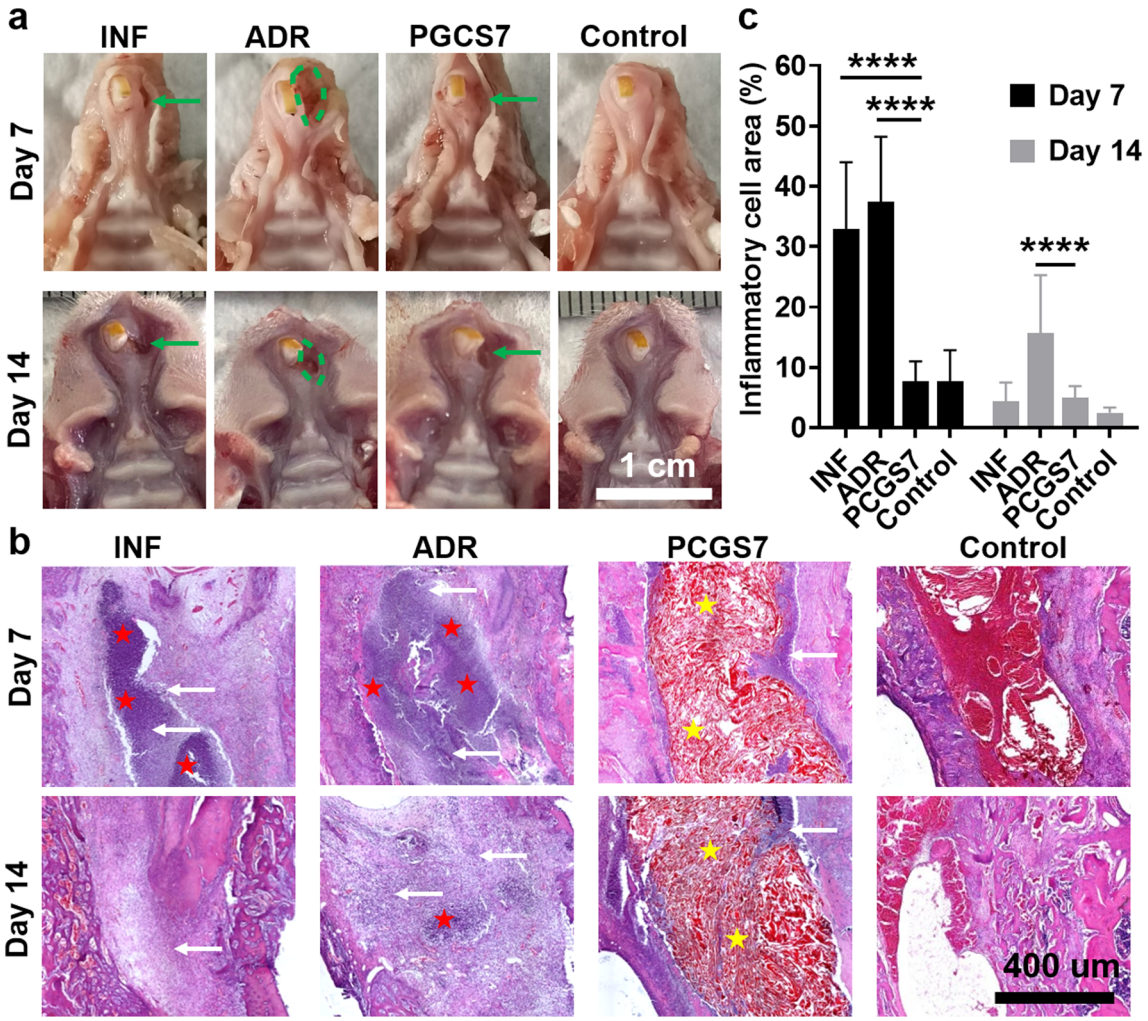

Fig. 7 *In vivo* wound-healing performance of PCGS7 in the rat infected-tooth-extraction model: (a) representative photographs (dashed green circle indicates highly exposed bone surface, green arrow indicates unexposed bone surface), (b) representative H&E staining analysis (white arrow indicates inflammatory cells, red pentagram indicates pyocyte mass, yellow pentagram indicates PCGS7 particles), and (c) inflammatory cell area (mean ± SD, $n \geq 3$, ****$p < 0.0001$, one-way ANOVA) of harvested maxilla samples in the INF, ADR, PCGS7, and control groups.

displayed an obviously reduced amount of filtrated inflammatory cells on day 14 in comparison with day 7. Meanwhile, the quantitative analysis revealed that the PCGS7 and INF groups exhibited similarly low relative areas of inflammatory cells on day 14 (Fig. 7c), which was significantly lower than that of the ADR group on day 14, which was consistent with the similarly good healing state (for a general view of the results, see Fig. 7a) of the PCGS7 and INF groups. Such H&E results of the PCGS7, INF, and ADR groups could be explained as follows: (1) as for the ADR group, the bacterial infection and associated inflammatory response were probably still on-going, which was due to the excessive hemostasis (corresponding to negligible blood clots) by adrenaline treatment and the resultant impairment of the antibacterial ability of the rats (endowed by the blood components);[37] (2) the PCGS7 group could overcome the aforementioned drawbacks of excessive hemostasis through the favorable antibacterial/anti-inflammatory properties of PCGS7, resulting in the limited infectious/inflammatory response of the tooth-extraction sockets; (3) it was speculated that the free bleeding (corresponding to abundant blood clots in the sockets; without the hemostat) in the INF group was conducive to suppressing infection through the immune system of healthy rats, which gave rise to the reduced infectious/inflammatory response from day 7 to day 14. To note, such a free bleeding state of the INF group would not be suitable for clinical practice, as it would not only cause the patients great suffering (prolonged bleeding and possible secondary bleeding) but also it would not be applicable for patients with low immunity and a possible high level of infection.

Notably, the inflammatory response of the tooth-extraction sockets in the PCGS7 group was higher than that in the control group on day 14 (Fig. 7b), which was consistent with the better healing quality of the control group than the PCGS7 group (for a general view of the results, see Fig. 7a). Owing to the high healing ability of healthy rats,[38,39] the fast

healing process of the uninfected tooth-extraction sockets (in the control group, representing an ideal healthy scenario) may be difficult to be exceeded by that of severely infected sockets receiving treatment (10^9 CFU of *S. aureus* per rat, in the PCGS7 group). Meanwhile, despite the degradability of chitosan/gelatin/PC, the PCGS7 filled in the tooth-extraction sockets only underwent a small amount of degradation from day 7 to day 14 (Fig. 7b and Fig. S7†), which may also be responsible for the higher inflammatory response of the PCGS7 group compared to the control group. Therefore, the future degradation process of PCGS7 remains to be further studied in large mammal animal models, to better evaluate its wound-healing performance in the infected-tooth-extraction model. Moreover, such a slow degradation in a rat model inspired us to further optimize the degradation rate of PCGS7 in future work *via* adjusting the sponge structure (*i.e.*, the molecular weights of chitosan/gelatin, the chemical modification of chitosan for new derivatives,[27] and the density of the sponge, which could be well tunable by the foaming process/stirring speed and feed concentrations). All the above results demonstrated that PCGS7 treatment outstripped the clinical adrenaline treatment in the infected-tooth-extraction model in terms of the healing quality and inflammatory response, which indicates it possesses certain application prospects in clinical scenarios (oral hemostasis and infection prevention after tooth extraction).

4. Conclusions

In summary, the multifunctional PCGS was designed and facilely prepared for hemostatic and infected wound therapy. Owing to the mixture components of chitosan and gelatin, PCGS possessed a highly porous interior morphology after a 'green' self-foaming condition and antibacterial ability against *S. aureus*. The incorporated PC endowed the PCGS with an enhanced blood-absorption/moderate surface charge (for good *in vitro* hemostatic property), and high antioxidant property, but slightly decreased antibacterial ability. PCGS achieved excellent hemorrhage-control performance in a rat femoral-artery-injury model, which realized an obviously reduced blood loss compared to commercial gelatin sponge. A rat infected-tooth-extraction model was also established to demonstrate the application prospect of PCGS in accelerating infected wound healing. Such a multifunctional hemostatic sponge, derived from total natural polymers and polyphenols, is worthy of further investigation for clinical utility as hemostatic and infected wound dressings.

Author contributions

Conceptualization, Y. S., Y. H., and F.-J. X.; Methodology, Y. S., T. M., Y. W., X. W., Y. H., and F.-J. X.; Investigation, Y. S., T. M., Y. W., J. L., Y. H., and F.-J. X.; Data curation, Y. S., T. M., Y. W., J. L., N. Z., and Y. H.; Validation, Y. S., T. M., Y. W., N. Z., and Y. H.; Writing – original draft, Y. S., T. M., X. W. and Y. H.; Writing – review & editing, Y. S., Y. H. and F.-J. X.; Funding acquisition, Y. S., Y. H. and F.-J. X.; Supervision, Y. H. and F.-J. X.

Conflicts of interest

The Beijing University of Chemical Technology has applied for a Chinese patent for the discussed PCGS with F.-J. X., Y. H., and T. M. listed as the inventors. The other authors declare no conflict of interest.

Acknowledgements

This work is financially supported by the National Natural Science Foundation of China (grant numbers: 52173114 and 82001101) and Beijing Outstanding Young Scientist Program (BJJWZYJH01201910010024).

References

1 X. Yang, W. Liu, N. Li, M. Wang, B. Liang, I. Ullah, A. Luis Neve, Y. Feng, H. Chen and C. Shi, *Biomater. Sci.*, 2017, **5**, 2357–2368.
2 L. Wang, X. You, C. Dai, T. Tong and J. Wu, *Biomater. Sci.*, 2020, **8**, 4396–4412.
3 Y. Wu, H. Wang, C. Fan, Z. Xu, B. Liu and W. Liu, *Mater. Horiz.*, 2020, **7**, 1091–1100.
4 H.-Q. Song, Y. Fan, Y. Hu, G. Cheng and F.-J. Xu, *Adv. Funct. Mater.*, 2021, **31**, 2005978.
5 H. Ye, J. Cheng and K. Yu, *Int. J. Biol. Macromol.*, 2019, **121**, 633–642.
6 S. Zhang, J. Li, S. Chen, X. Zhang, J. Ma and J. He, *Carbohydr. Polym.*, 2020, **230**, 115585.
7 R. Liu, L. Dai, C. Si and Z. Zeng, *Carbohydr. Polym.*, 2018, **195**, 63–70.
8 Y. Liang, Z. Li, Y. Huang, R. Yu and B. Guo, *ACS Nano*, 2021, **15**, 7078–7093.
9 Z. Xu, W. Tian, C. Wen, X. Ji, H. Diao, Y. Hou, J. Fan, Z. Liu, T. Ji, F. Sun, D. Wu and J. Zhang, *Nano Lett.*, 2022, **22**, 6350–6358.
10 J.-Y. Liu, Y. Hu, L. Li, C. Wang, J. Wang, Y. Li, D. Chen, X. Ding, C. Shen and F.-J. Xu, *Adv. Sci.*, 2020, **7**, 2002243.
11 Z. Zhang, G. Kuang, S. Zong, S. Liu, H. Xiao, X. Chen, D. Zhou and Y. Huang, *Adv. Mater.*, 2018, **30**, 1803217.
12 J.-Y. Liu, Y. Li, Y. Hu, G. Cheng, E. Ye, C. Shen and F.-J. Xu, *Mater. Sci. Eng. C*, 2018, **83**, 160–168.
13 Z. Chen, L. Han, C. Liu, Y. Du, X. Hu, G. Du, C. Shan, K. Yang, C. Wang, M. Li, F. Li and F. Tian, *Nanoscale*, 2018, **10**, 20234–20245.
14 L. Tan, X. Zhou, K. Wu, D. Yang, Y. Jiao and C. Zhou, *Int. J. Biol. Macromol.*, 2020, **159**, 304–315.
15 S. Kumbargere Nagraj, E. Prashanti, H. Aggarwal, A. Lingappa, M. S. Muthu, S. Kiran Kumar Krishanappa and H. Hassan, *Cochrane Database Syst. Rev.*, 2018, **3**, CD011930.

16 E. Iwata, A. Tachibana, J. Kusumoto, T. Hasegawa, R. Kadoya, Y. Enomoto, N. Takata and M. Akashi, *Oral Maxillofac. Surg.*, 2022, **26**, 641–648.
17 N. J. McCormick, U. J. Moore and J. G. Meechan, *Dent. Update*, 2014, **41**, 290–296.
18 J. Mamoun, *J. Korean Assoc. Oral Maxillofac Surg.*, 2018, **44**, 52–58.
19 D. C. Bowe, S. Rogers and L. Stassen, *J. Ir. Dent. Assoc.*, 2011, **57**, 305–310.
20 J. Wang, M. Bie, W. Zhou, B. Xie and Z. Sun, *Carbohydr. Polym.*, 2019, **212**, 11–20.
21 P. Zhou, L. Zhang, W. Li, S. Zhang, L. Luo, J. Wang and B. Sun, *J. Funct. Foods*, 2018, **49**, 85–95.
22 K. Quan, G. Li, L. Tao, Q. Xie, Q. Yuan and X. Wang, *ACS Appl. Mater. Interfaces*, 2016, **8**, 7666–7673.
23 L. Long, Y. Fan, X. Yang, X. Ding, Y. Hu, G. Zhang and F.-J. Xu, *Chem. Eng. J.*, 2022, **444**, 135426.
24 Y. Qin, J. Wang, C. Qiu, Y. Hu, X. Xu and Z. Jin, *ACS Sustainable Chem. Eng.*, 2019, **7**, 17379–17389.
25 X. Bao, J. Zhao, J. Sun, M. Hu and X. Yang, *ACS Nano*, 2018, **12**, 8882–8892.
26 Y. Sun, K. Kaur, K. Kanayama, K. Morinaga, S. Park, A. Hokugo, A. Kozlowska, W. H. McBride, J. Li, A. Jewett and I. Nishimura, *J. Biol. Chem.*, 2016, **291**, 20602–20616.
27 Q. Hu and Y. Luo, *Carbohydr. Polym.*, 2016, **151**, 624–639.
28 D. Zhang, Z. Xu, H. Li, C. Fan, C. Cui, T. Wu, M. Xiao, Y. Yang, J. Yang and W. Liu, *Biomater. Sci.*, 2020, **8**, 1455–1463.
29 H. A. Lee, E. Park and H. Lee, *Adv. Mater.*, 2020, **32**, 1907505.
30 Y. Sun, X. Jing, Y. Liu, B. Yu, H. Hu, H. Cong and Y. Shen, *Carbohydr. Polym.*, 2023, **300**, 120298.
31 F. Devlieghere, A. Vermeulen and J. Debevere, *Food Microbiol.*, 2004, **21**, 703–714.
32 G.-X. Xia, Y.-M. Wu, Y.-F. Bi, K. Chen, W.-W. Zhang, S.-Q. Liu, W.-J. Zhang and R.-H. Liu, *Chin. J. Polym. Sci.*, 2021, **39**, 133–146.
33 Y. Wu, G. Xia, W. Zhang, K. Chen, Y. Bi, S. Liu, W. Zhang and R. Liu, *J. Mater. Chem. B*, 2020, **8**, 9173–9196.
34 H. Gradišar, P. Pristovšek, A. Plaper and R. Jerala, *J. Med. Chem.*, 2007, **50**, 264–271.
35 T. Zhu, J. Wu, N. Zhao, C. Cai, Z. Qian, F. Si, H. Luo, J. Guo, X. Lai, L. Shao and J. Xu, *Adv. Healthcare Mater.*, 2018, **7**, 1701086.
36 A. Hokugo, K. Kanayama, S. Sun, K. Morinaga, Y. Sun, Q. Wu, H. Sasaki, H. Okawa, C. Evans, F. H. Ebetino, M. W. Lundy, K. Sadrerafi, C. E. McKenna and I. Nishimura, *Bone*, 2019, **123**, 115–128.
37 M. Taberner-Vallverdú, M.-Á. Sánchez-Garcés and C. Gay-Escoda, *Med. Oral Patol. Oral Cir. Bucal.*, 2017, **22**, e750–e758.
38 J. S. Hassumi, G. Mulinari-Santos, A. L. D. S. Fabris, R. G. M. Jacob, A. Goncalves, A. C. Rossi, A. R. Freire, L. P. Faverani and R. Okamoto, *J. Appl. Oral Sci.*, 2018, **26**, e20170326.
39 E. S. Willett, J. Liu, M. Berke, P. J. Giannini, M. Schmid, Z. Jia, X. Wang, X. Wang, K. Samson, F. Yu, D. Wang, A. Nawshad and R. A. Reinhardt, *J. Periodontol.*, 2017, **88**, 799–807.

